Journal of the European Ceramic Society 20 (2000) 481–488

Effect of impact angle on glass surfaces eroded by sand blasting

Said Bouzid*, Nourredine Bouaouadja

Laboratoire Matériaux, IOMP, Université Ferhat Abbas, Sétif 19000, Algeria

Received 10 February 1999; received in revised form 24 April 1999; accepted 11 May 1999

Abstract

In a previous work, we studied the effects of sand blasting on the roughness, the optical transmission and the mechanical strength of a soda lime glass for sand blasting durations up to 150 min and under a constant impact angle of 90°. In the present work, we examine the effect of impact angles (30 to 90°) for relatively small durations up to 60 min on the surface roughness and the optical transmission. The roughness increases and tends towards a plateau, while the optical transmission decreases and tends towards a threshold estimated at about 50% of the initial transmission. We noticed that the samples erosion damage becomes weaker for impact angles less than 90° (90° angle corresponds to the flux normal to the samples). Microscopic observations reveal that the damage is similar to that of sharp indentation damage type Vickers indentation. There is formation of a plastic imprint with radial cracks and some scaling caused by the development of lateral cracks that extend and curve up to the surface. From the expression of the damage rate as defined in the literature, we introduced a function relating the impact angles and the sand blasting durations to the optical transmission. The experimental data obtained seem to fit quite well to the proposed function.

Keywords: Glass; Optical properties; Sand blasting; Surfaces

1. Introduction

In most applications, the glass surface is exposed to a variety of external agressive conditions such as corrosion, chemical reactions and mechanical damage. The erosion of brittle materials by particle impacts is caused by localised cracking. The intersection of cracks with each other and with the surface leads to material removal. It is known that erosion of materials depends strongly on the impact angle. For brittle materials, the erosion rate decreases markedly as the impact angle decreases from 90° (flow normal to the surface), while for ductile materials the erosion rate presents a maximum at an impact angle of about 30°.[1]

Erosion of glass by sand impact has not been intensively studied the last years, in comparison with other brittle materials. Ritter et al.[2] have reported that the erosion damage in soda-lime glass by SiC particles can be modelled very well by indentation fracture mechanics. For soda-lime glass, erosion produces numerous small chipped zones. Ludwig and Stoner[3] have undertaken a quantitative study of abrasion resistance of optical coatings and surfaces by falling sand abrasive. They have proposed a model for understanding the abrasion of surface. The model is in good agreement with their experimental data. In contrast to glasses, the erosion by solid particles of some ceramics (Al_2O_3[4]) and composite materials (Al_2O_3/SiC,[5] SiC/Si_3N_4,[6] Al_2O_3/ZrO_2,[7] etc) has been widely covered these last years. A particular attention has been devoted to the study of erosion mechanisms. Sparks and Hutchings[8] have investigated the mechanisms of material removal during the erosive wear of a glass-ceramic. It was found that different mechanisms occurred in dependence with particle shape, impact velocity and impact angle. According to the authors, their work indicates that laboratory erosion testing of glass ceramic and other brittle materials should reflect the conditions present in practice. In the case of sintered alumina, Ritter et al.[2] have shown that the erosion damage was characterised by pits created through intergranular chipping. This erosion could not be explained by indentation fracture theory.

According to literature,[9,10] it is well established that erosion of brittle materials by hard particles results from elastic–plastic fracture. This fracture is characterised

* Corresponding author.

0955-2219/00/$ - see front matter
PII: S0955-2219(99)00140-5

from the contact area between the impacting particle and target. In the case of sharp particles, there is subsurface lateral cracks propagating outward from the base of the contact zone on planes nearly parallel to the surface, and radial cracks propagating from the contact zone normal to the surface. The lateral cracks are considered responsible for material removal and the radial cracks the main source of strength degradation.[2]

In the last years, several authors[11,12] studied the erosion of brittle materials using different approaches. They clearly showed, for example, the importance of the parameters intervening in the erosion process in the case of a brittle surface impacted by solid particles. These parameters were essentially:

- the nature and properties of the particles (size, shape, hardness, toughness);
- the nature and properties of the surface target (hardness, toughness, state of superficial stresses);
- the effect of the environment (speed of the flow, impact angles, temperature variations).

The erosion by sand particles of brittle materials like glass is a very regular phenomenon in the Saharian regions. The progressive loss of material on the surface affects both the mechanical resistance and the optical transmission.[13] In several cases, the decrease of the optical transmission becomes very inconvenient for the use of glass.

In this study, we simulated in the laboratory the effect of sand blasting on the roughness and on the optical transmission of a soda-lime glass. The varying parameters are the different impact angles between 30 and 90° and short durations up to 1 h. These durations are smaller than the saturation time shown in a previous work to be greater than 150 min.[13]

2. Test conditions

In order to simulate the effects of the sandstorm durations and the impact angles on the properties of a soda-lime glass surface, a sand blower apparatus was employed (Fig. 1). The erosion tests were carried out with a stationary sample impacted by sand particles accelerated in an air stream by a ventilator. We have used a nozzle diameter $d = 4$ cm. The sand feed during the erosion tests was fixed constant at about 1.58 g/s.

It was reported in the literature that the particles velocity can be measured using different methods: light speed photography,[14] double rotating disks[15,16] or calculation by numerical methods.[14] All these methods concern the test conditions with high speed generally more than 100 m/s. In our case, the air blower velocity was measured using an anemometer and was found to be 16.6 m/s which represents a mean velocity of sand

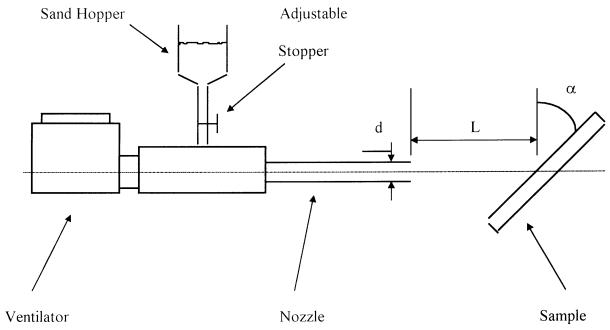

Fig. 1. Schematic illustration of the sand blower used and the orientation α of the specimen.

blasting in the Saharian regions. It is evident that the flux velocity obtained by the anemometer does not correspond to the sand particles velocity. It was not determined because of the complexity related to the variations of the sand nature, size and shape. In this work, we maintained constant the air flux velocity for all the tests done.

According to Davies,[17] a circular flow emerging from a cylindrical nozzle with a diameter d presents a divergent cone whose apex angle 2δ is given by experience as being between 25 and 30°. The cone can be divided into four distinctives zones whose lengths depend on the nozzle diameter d. In our study, we have opted for the first zone ($0 < L < 6.2d$) where the velocities are found uniform and equal to the air flow velocity into the nozzle. On the basis of this assumption, the distance L between the pipe nozzle and the specimens was adjusted to 24 cm.

The roughness measurements were made with a surface profilometer "Hommel Tester T20 Digital Computer". The optical transmission measurements were carried out on washed and dried specimens using a microdensitometer "MD 100 type Carl Zeiss". The roughness and the transmission values obtained in this work represent mean values of five measurements. Finally, the eroded surfaces were examined with a "Neophot 21" optical microscope. During the tests, the impact angle 90° corresponds to sample position perpendicular to the air flow.

The samples were prepared from a soda-lime glass sheet of local production (ENAVA firm). The dimensions used were $140\times140\times3$ mm^3. The Poisson's ratio is 0.22, the Young's modulus is 72 GPa and the fracture strength is 87.5 MPa.[18] The surfaces were tested in the as received state which present a total roughness of 0.242 μm and an initial optical transmission of 91.5%. For each tested specimen, total roughness Rt and optical transmission T of the sand blasted surface were measured following the median line on every step of 10 mm from the edge (see Fig. 7). On the figures showing the evolution of the roughness and the optical transmission with durations and impact angles, we have used

the maximum values Rt and T obtained in the center of the specimens.

The sand employed comes from the region of Biskra (North of Sahara, Algeria). During the tests, it was washed, dried and sifted in order to eliminate small particles. The sand grains size varies between approximately 100 and 800 μm. Fig. 2 shows a sample of the sand used in this study. We can observe that the shape of the particles is very irregular. There are rounded (arrows a) and angular grains (arrows b) with different sizes. We can also notice that there is a predominance of sharp grains with different sharp angles (arrows b) which could be simulated by sharp indenters (Vickers or Knoop indenters). Vickers microhardness of the sand grains, which were embedded in a thermosetting resin and polished, was measured at a 0.5 N load. The mean value was 7.32 ± 2.94 GPa. This microhardness scattering is probably due to the chemical nature of the grains which contain different amounts of oxides.

The erosion tests were conducted at the ambient temperature (≈26°C) in the following conditions:

• fixed parameters:	speed of the air flow: 16.6 m/s (≈60 km/h) mass flow: 1.58 g/s distance between the nozzle and the target: 24 cm size range of the sand grains: ≈(100÷800) μm
• variable parameters:	durations $t = 5$, 10, 20, 40, 60 min impact angles $\alpha = 30$, 50, 70, 90°.

3. Results and discussion

3.1. Roughness

Examination of the specimen after sand blasting tests shows that when the glass surface is normal to the air flow, the damaged surface is circular, and when the area of contact is inclined, we have an assymetrical eroded surface (an elliptical form with a larger side) as presented in Fig. 7. When the length $L = 4d$, Chevalier[19] confirms that the particles continue their trajectory without being deviated onto the area around the surface.

An example of the obtained roughness profiles established for 10, 30 and 60 min under an impact angle of 90° is given in Fig. 3. We can clearly observe that the impact number and the depth of superficial defects increase during the sand blasting. The larger the time, the larger is the damage. For 10 min, the defects are less numerous and less deep (about 0.65 μm). For 30 min, the surface damage increases in density and in depth which reaches 1.87 μm. We can notice that there is a begining of defects interaction which activates the erosion mechanism. After 60 min of sand blasting, the interactions between defects increase in size because of the repeated grain impacts and consequently the residual stresses cumulated on the surface. The level differences between the crests and the hollows increase, and the roughness tends towards 4.0 μm.

The micrographs in Fig. 4 show a glass surface eroded by sand particles for 30 and 60 min. We can clearly observe that the density of the flaws generated by the sand grains impacts increases with the sand blasting durations. There is formation of plastic imprint[20] with radial cracks and some scaling. For 30 min, there is formation of small damaged zones which extend probably under the repeated sand impacts. For 60 min, the defects density increases again and the formation of damaged zones tends to be generalised on all the eroded surface with a regular distribution. The erosion of the sand blasted surfaces occurs with a loss of matter by scaling.

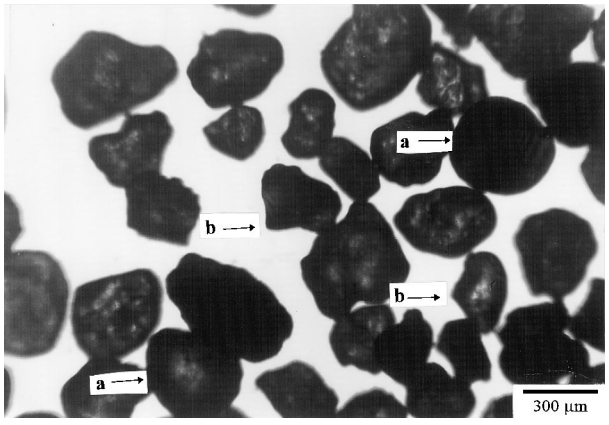

Fig. 2. Optical micrograph of the sand used in this study. Arrows a and b show, respectively, the rounded and the sharp particles.

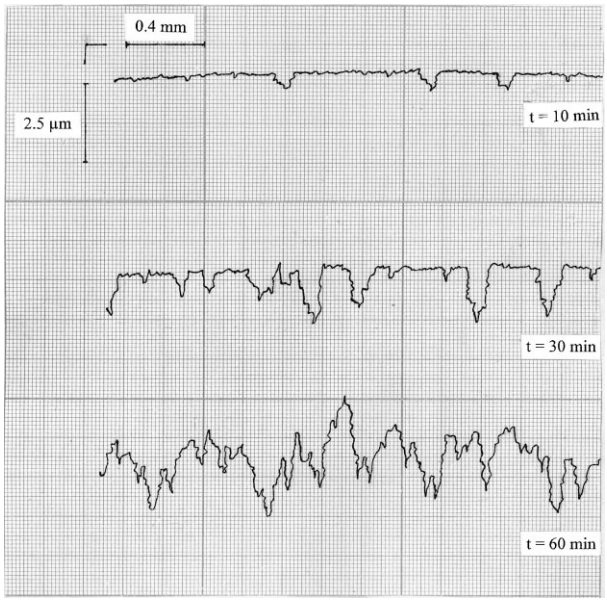

Fig. 3. An example of the roughness profiles obtained after 10, 30 and 60 minx of sand blasting showing the increase of the damage.

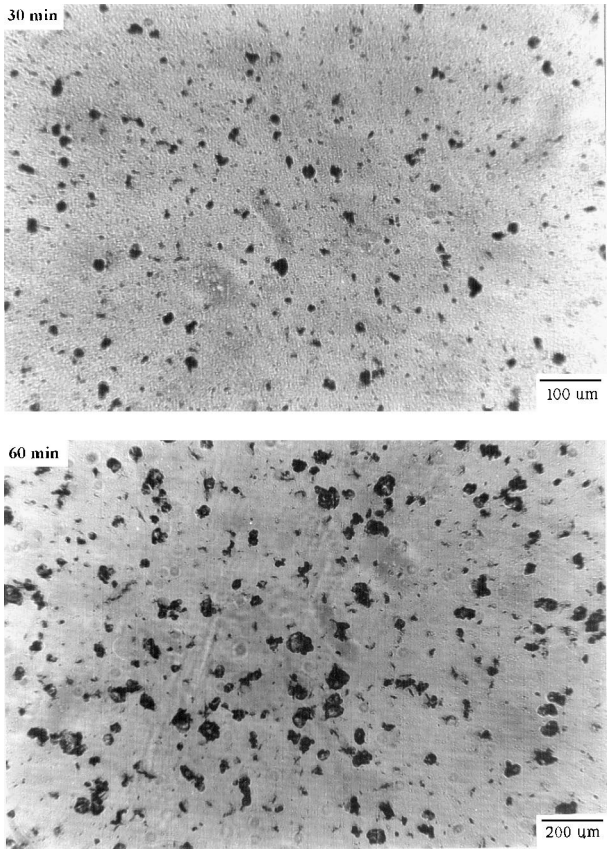

Fig. 4. Optical micrographs showing the damage caused on the glass surfaces eroded during 30 and 60 min under an impact angle of 90°.

Fig. 5 shows some details of typical surface damage induced by sand impacts. The damage is essentially produced by scaling with formation and extension of lateral cracks corresponding to sharp indentation damage. We can see, for example, the trace of subsurface lateral cracks which propagate outward from the base of the contact zone on planes nearly parallel to the surface (arrow a), the cracks which curved up and intersect the glass surface (arrow b) and finally the morphology of the scales after detachment (arrow c).

Fig. 6 shows some imprints and the radial cracks caused by sharp sand particles. We can clearly observe that the cracking systems of the radial cracks present different branchings. As shown by Franco and Roberts[21] in the case of eroded alumina, we can see that in some areas cracks associated with damage zones are interconnected. Besides the scales detached from single impact sites, some amounts of material are removed from the surface when two or more impact sites are close to each other, so that the crack system from the impact events intersect. Arrows in Fig. 6 show a typical interaction between two adjacent impacts: a big imprint (A) similar to a vickers indentation, and a smaller imprint (B) located at about an angle of 45°. Lateral crack of the big imprint (scale) interact with the radial cracks of the small imprint and influence their orientation.

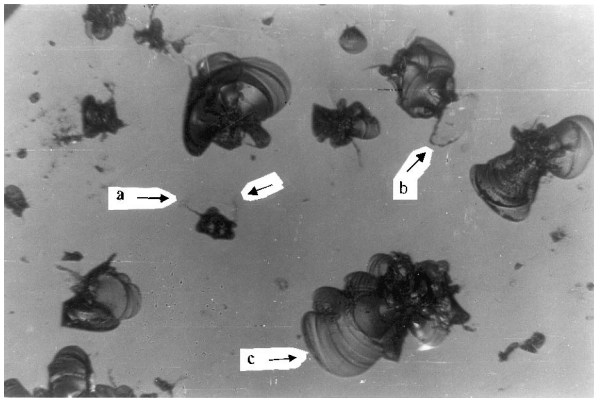

Fig. 5. Micrograph showing some details of the lateral cracks formation (×320): arrow a, trace of lateral crack; arrow b, intersection with the surface; arrow c, morphology after detachment of the scale.

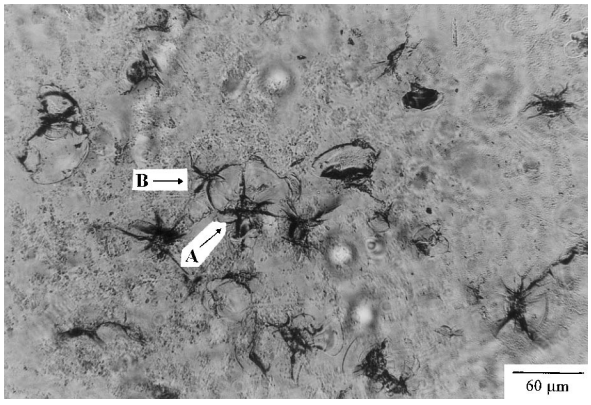

Fig. 6. Micrograph showing some details of microcracks obtained for $t = 30$ min, $\alpha = 90°$. Arrows indicate crack interaction between a big imprint (A) and a small imprint (B).

The measurement of the roughness profile after some sand blasting durations is obtained following X axis in the median line using a step of 10 mm from the specimen edge (see Fig. 7). The distribution of the total roughness Rt established in function of sand blasting durations for different impact angles is plotted in Fig. 8. It indicates that all the roughness curves are nearly symmetrical in X axis and present a maximum in the central zone of the sand blasted surface ($X = 0$ mm). Near the edges, Rt tends towards very weak values. The curves level decreases regularly with the sand blasting durations and from 90° to 30° impact angles. In average, the values pass from 3.92 µm for 90° to 0.78 µm for 30°. We could notice that for the orientation 90°, the curves present a nearly flat maximum near the center. This lets us think that the flux of particles is essentially centered in a zone of about 20 mm diameter and that in outside of this zone, there is a scattering of sand grains which decreases sensitively towards the specimens edges. The central flow of particles after impact interferes with the particles arriving at relatively low speed at the top of

the eroded surface. This can be attributed to the air jet capacity to move towards the high edge of the samples. Moreover, it can be supposed that a particle striking the surface with an angle α rebounds with the same angle α and tends to move the high edge of the sample. When the particles which have rebounded interfere with the particles coming towards the summit of the ellipse, the surface damage is reduced on the upper side of the ellipse. The flat maximum observed for 90° impact angle corresponds to the central zone of the surface which is more severely and uniformly damaged in comparison with the remaining zones. Fig. 9 illustrate the roughness repartition on the glass specimen. The impacting sand particles are normally oriented towards the surface. The normal forces give a uniformly damaged zone. In the remaining zones where tangential component of the forces intervene, the roughness decrease is due to the apex angle 2δ. The roughness decreases as the apex angle increases.

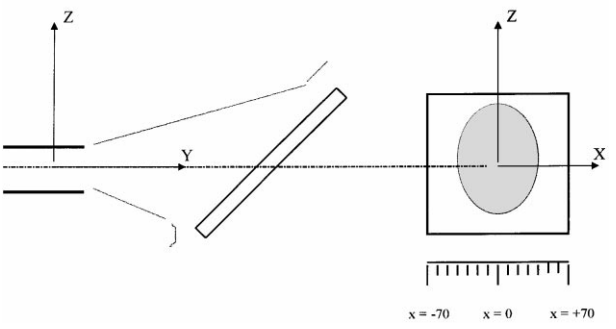

Fig. 7. Schematic illustration of the erosion jet striking the inclined surface and the main elliptical damaged zone with the measurement positions X.

Thereafter, we have established the variation of the total roughness versus impact angles for different sand blasting durations (Fig. 10). We can observe that from 30°, the roughness increases linearly with impact angle and varies sensitively with sand blasting durations.

Fig. 11 shows the variations of the total roughness versus the sand blasting durations for different impact angles. We can notice that *Rt* increases sharply for the

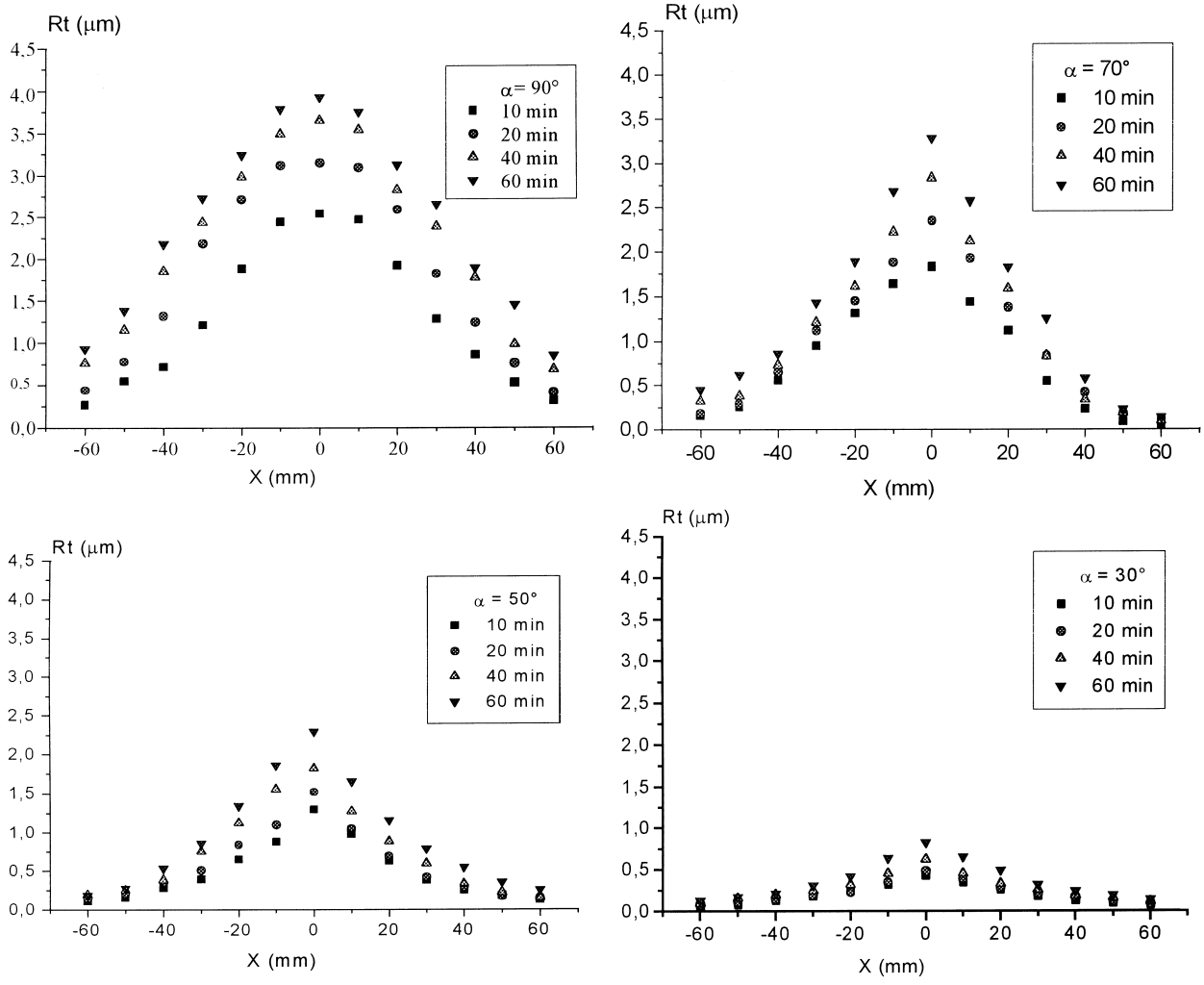

Fig. 8. Variations of the total roughness *Rt* versus the measurement positions X for different durations and for 90°, 70°, 50° and 30° impact angles.

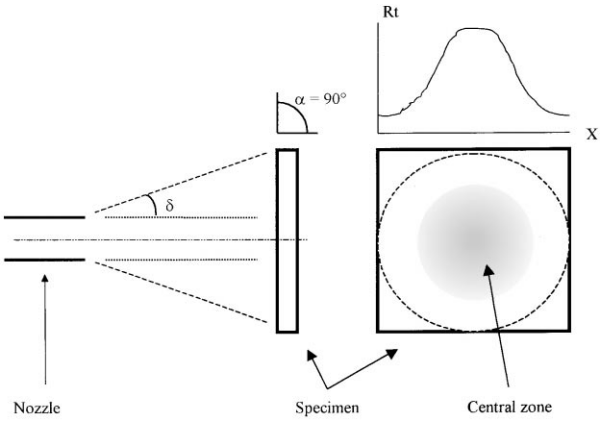

Fig. 9. Illustration of the roughness repartition showing the central zone severely and uniformly eroded comparing to the remaining zones.

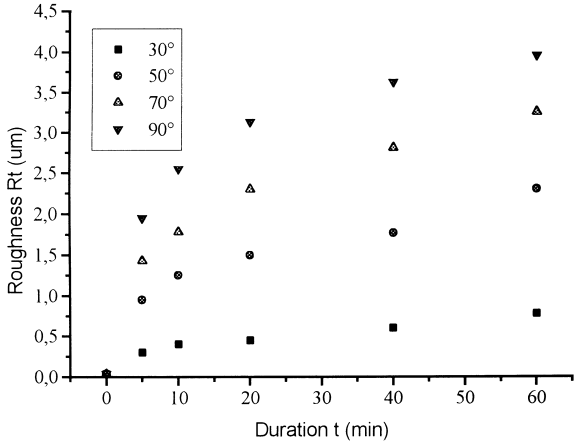

Fig. 11. Variation of the total roughness *Rt* versus the sand blasting durations for different impact angles.

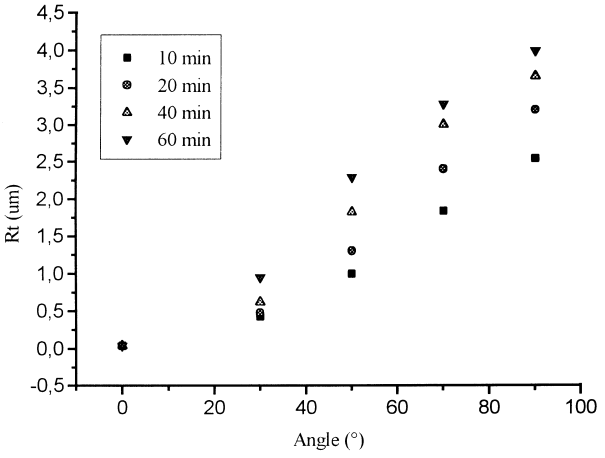

Fig. 10. Variation of the total roughness *Rt* versus the impact angles for different durations.

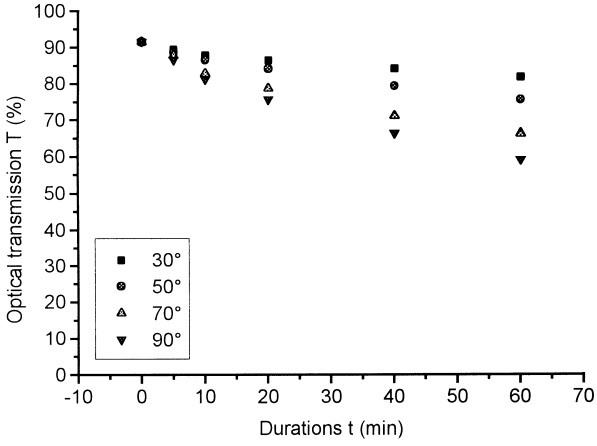

Fig. 12. Variation of the optical transmission versus sand blasting durations for different impact angles.

short durations (until 20 min) and smoothly for the relatively large durations. This can be explained by the fact that from 20 min duration, the interaction between defects contributes to the homogenisation of the roughness relief stabilising the level differences between the crests and the hollows. It is apparent that the impact angle 90° manifest the maximum roughness because the normal force of the projectiles is higher and consequently the damage is more important.

3.2. Optical transmission

In the same way as for the roughness measurements, the determination of the optical transmission was first raised in the median line of the eroded surface. Fig. 12 shows the variation of the optical transmission versus the sand blasting durations for different impact angles. We can see that the optical transmission decreases gradually with the sand blasting durations from 30° to 90°. For relative long duration (60 min), the optical transmission decrease passes from about 10.4% for the 30° orientation to 36.6% for 90°. This loss is mainly due to the light scattering and light reflection caused by the surface damage under the repeated impacts of the sand grains.

In general under the same test conditions and for the same sand blasting duration, the optical transmission is minimum for an impact angle of 90°. With this position, the normal force and the kinetic energy of the particles are maximum. This orientation can be considered as the most favourable for the damage by solid particles of the brittle surfaces.

According to Fig. 12, the optical transmission reached under an impact angle of 90° and for a duration of 60 min is about 59% comparing to the initial transmission ($T_0 = 91.5\%$). In general, we could obtain a same state of damage by combining the two parameters: sand

blasting duration and impact angle. Thus, a damage produced under an angle of 90° for a duration t is equivalent to the same damage produced under an inferior impact angle but for a duration t' relatively longer. On the basis of this assumption, we could easily imagine that for a time sufficiently long, all the curves of Fig. 12 tend toward a threshold value of the optical transmission. In our case, this threshold value is estimated to about 48% which is nearly half the value of the initial optical transmission T_0 ($\approx 0.5\,T_0$). This last value agrees with the one obtained in a nearly similar conditions in a previous work (≈52%) for a sand blasting duration of 150 min.[13]

3.3. Surface damage

It is well known that damage influences the glass surface through the loss of transparency and the reduction of mechanical strength. In the case of glass erosion by sand blasting, damage can be described as a progressive deterioration of the material in function of the test parameters such as the sand blasting durations, the flux orientation, the flux speed, the size and the shape of the sand particles, etc In order to estimate the damage effects on the properties of glass, we introduce a damage-transmission function. First, we suppose the glass is homogeneous and that the surface do not contain any major defects capable to initiate glass degradation. After sand blasting tests, the surface state changes and becomes damaged by particle impacts and by interactions between the surface flaws. Knowing that sand blasting erosion is a surface damage, the damage rate can be defined by the ratio S_D/S_0 (S_0 is the initial surface before exposure to sand blasting and S_D is a damaged surface). The damage variable D can be expressed by:[22]

$$D = S_{\mathrm{D}}/S_0 \tag{1}$$

Damage is defined as a scalar parameter $(0 \leqslant D \leqslant 1)$ such that $D = 0$ corresponds to the undamaged surface, $D = 1$ corresponds to the completely damaged surface, and intermediate values of D correspond to intermediate damage states of the surface.

The relationship mentioned above could be verified experimentally, either by direct measurements (microscopic observations) or by indirect measurements (transmitted or reflected light methods). From the expression of the transmission rate defined for an undamaged glass surface as $T = I_T/I_0$ (transmitted intensity over incident intensity), we introduced the damage effect quantifying the undamaged surface ratio by $(1 - D)$. In this case, the transmission T_D of a damaged surface can be expressed as:

$$T_{\mathrm{D}} = T_0(1 - D) \tag{2}$$

where T_0 is the optical transmission of the initial surface.

According to this relation:

- when D tends towards 0 (undamaged state), T_{D} tends towards T_o;
- when D tends towards unity (saturated state), T_{D} tends towards 0.

In practice, the optical transmission never reach completely the zero value even for the saturation state. This is well known for ground and abraded glasses. For this reason, we proposed instead the expression (5).

The damage of a glass surface submitted to sand blasting during a time t under an impact angle of 90° can be expressed as an exponential function [Eq.(3)]. This equation is a global form obtained from Eq. (2) and from experimental values of the optical transmission for different durations. It was proposed by fitting the evolution of the damage ratio with the sand blasting duration (Fig. 13):

$$D = 1 - \exp(-\chi \cdot t) \tag{3}$$

χ is a constant determined by fitting the optical transmission variations or by calculation knowing the transmission values before and after sand blasting. For different impact angles α, we have a power function defining χ as:

$$\chi = 0.28.10^{-4}(\alpha^{1.5}) \tag{4}$$

By substituting Eq. (3) in Eq. (2) and replacing χ by its expression, we obtain a new function which permits to describe the evolution of the optical transmission T_{D} of a glass eroded by sand blasting in function of the durations t and the impact angles α:

$$T_{\mathrm{D}} = A.T_0\left[1 + \exp(-0.28.10^{-4}(\alpha^{1.5}).t)\right] \tag{5}$$

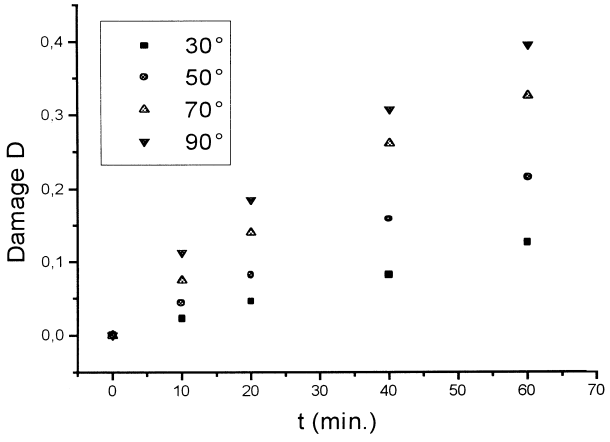

Fig. 13. Variation of the damage versus the sand blasting durations for different impact angles.

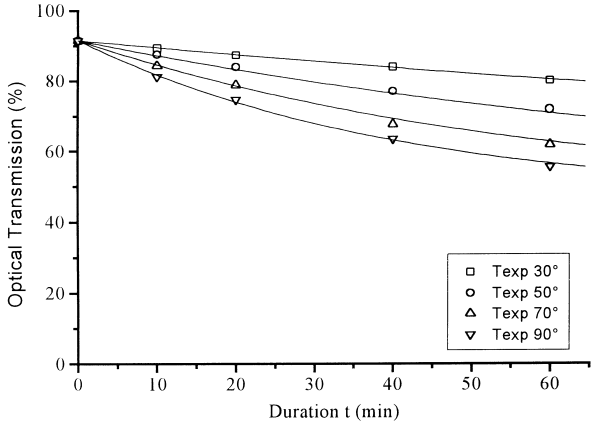

Fig. 14. Comparison of the transmission variations versus the sand blasting durations using Eq. (5) and the experimental data obtained for different impact angles.

where A is a constant depending on the test conditions. It was previously determined as being equal to 0.5 (c.f. Section 3.2).

We noticed that the Eq. (5) fits quite well the experimental data for the case of the optical transmission in function of the sand blasting durations for different angles (Fig. 14). Knowing the complexity of the sand blasting erosion phenomenon, it is recommended to associate other essential parameters such as the flux velocity and the grains properties in order to obtain a model that describes closely the real conditions.

4. Conclusion

In this work, we simulated the effect of sand blasting on the surface of a soda-lime glass. We have examined the influence of the impact angle and the sand blasting duration on the total roughness and on the optical transmission. We noticed that the roughness increases proportionally to the sand blasting durations, when the impact angle tends toward 90°. Microscopic observations allowed to see the evolution of the damage caused on the glass surface. This damage appeared like a limited zone which spread gradually on all the surface in function of durations and orientation of the sand flux.

The effect of the impact angle on the optical transmission was also put in evidence. This last decreased regularly with the durations and with the impact angle becoming minimal for an angle of 90°. Finally, we introduced a damage function from which we established a formula that allows to express the evolution of the optical transmission for a damaged glass with the durations and the flux orientation. This formula agrees well with the experimental data.

References

1. Lawn, B. R., *Fracture of Brittle Solids*, 2nd edn. Cambridge University, Cambridge, UK, 1993 pp. 302–304.
2. Ritter, J. E., Strzepa, P., Jakus, K., Rosenfeld, L. and Buckman, K. J., Erosion damage in glass and alumina. *J. Am. Ceram. Soc.*, 1984, **67**, 769–774.
3. Ludwig, M. A. and Stoner, R. B., Quantitative abrasion resistance of optical coatings and surfaces. *J. Appl Phys.*, 1986, **60**, 4277–4280.
4. Wada, S. and Watanabe, N., Solid particle erosion of brittle materials — Part 4: the erosive wear of thirteen kinds of commercial Al_2O_3 ceramics. *J. Ceram. Soc. Jpn*, 1987, **95**, 835–840.
5. Wada, S., Watanabe, N. and Tani, T., Solid particle erosion of brittle materials — Part 6: the erosion wear of Al_2O_3/SiC composites. *J. Ceram. Soc. Jpn*, 1988, **96**, 111–118.
6. Wada, S., Watanabe, N., Tani, T. and Kamagaito, O. Erosion wear of Si_3N_4/SiC composites. In *MRS Int. Meeting on Adv. Mater*. Mater. Res. Soc., Pittsburgh, PA, 1989, pp. 481–490.
7. Wada, S. and Watanabe, N., Solid particle erosion of brittle materials — Part 3: the interaction with material properties of target and that of impingement particle on erosive wear mechanism. *Yogyo Kyokai Shi.*, 1987, **95**, 573–578.
8. Sparks, A. J. and Hutchings, I. M., Transitions in the erosive wear behaviour of a glass ceramic. *Wear*, 1991, **149**, 99–110.
9. Evans, A. G., Gulden, M. E. and Rosenblatt, M., Impact damage in brittle materials in the elastic–plastic response regime. *Proc. R. Soc. London, Ser. A*, 1978, **361**, 343–365.
10. Wiederhorn, S. M. and Hockey, B. J., Effect of material parameters on the erosion resistance of brittle materials. *J. Mat. Sci.*, 1983, **18**, 766–780.
11. Wellman, R. G. and Allen, C., *Wear*, 1995, **186–187**, 117–122.
12. Wiederhorn, S. M. and Lawn, B. R., Strength degradation of glass impacted with sharp particles: I. annealed surfaces. *J. Am. Ceram. Soc.*, 1979, **62**, 67–70.
13. Bousbaa, C., The effect of durations on the properties of a window glass. *Glass Techn.*, 1998, **39**, 24–26.
14. Lloyd, D. M., Rogers, E. A., Oakey, J. E. and Pittaway, A. J., Metal wastage in fluidised-bed combustors. *Mat. Sci. Eng.*, 1987, **88**, 295–301.
15. Ruff, A. W. and Ives, L. K., Measurement of solid particle velocity in erosive wear. *Wear*, 1975, **35**, 195–199.
16. Levy, A. V., The role of plasticity in erosion. In *Proc. 5th Inter. Conf. on Erosion by Solid and Liquid Impact* (field edn). University of Cambridge, 1979, pp. 39/1–39/10
17. Davies, J. T., *Turbulence Phenomena*. Academic Press, 1972, p. 66.
18. Hamidouche, M., Louahdi, R., Bouaouadja, N. and Osmani, H., The fracture toughness of soda-lime glass. *Glass Techn.*, 1994, **35**, 183–185.
19. Chevalier, P. and Vannes, A. B., Effect on a sheet surface of an erosive particle jet upon impact. *Wear*, 1995, **184**, 87–91.
20. Buijs, M., Erosion of glass as modelled by indentation theory. *J. Am. Ceram. Soc.*, 1994, **77**, 1676–1678.
21. Franco, A. and Roberts, S. G., The effect of impact angle on the erosion rate of polycrystalline α-Al_2O_3. *J. Eur. Ceram. Soc.*, 1998, **18**, 269–274.
22. Lemaitre, J., Micro-mechanics of crack initiation. *Int. J. Fract.*, 1990, **42**, 87–99.